Zinc oxide nanorods effect in micro structural and mechanical characteristics of aluminium composite material

Neeraj Kumar Bhoi[1,*], Harpreet Singh[2], Saurabh Pratap[3], Sumsun Naher[4], Pramod K Jain[5]

[1,2]Department of Mechanical Engineering, Indian Institute of Information Technology Design and Manufacturing, Jabalpur, Madhya Pradesh, India

[3,5]Department of Mechanical Engineering, Indian Institute of Technology Varanasi, Uttar Pradesh, India

[4]Department of Mechanical Engineering and Aeronautics, City, University of London, London, United Kingdom

[5]Department of Mechanical and Industrial Engineering, Indian Institute of Technology, Roorkee, Uttarakhand, India

Email Id: [1]neerajbitd@gmail.com, [2]hps.dme@gmail.com, [3]s.pratapiitkgp@gmail.com, [4]sumsun.naher.1@city.ac.uk, [5]pkjain123@gmail.com

*Corresponding author

ORCID iD: *https://orcid.org/0000-0002-7805-3335

Abstract:

In the present study, aluminium zinc oxide (Al-ZnO) nanorods composites with 3.5 and 5 wt.% ZnO in Al were manufactured using powder metallurgy and microwave hybrid sintering. A fairly uniform reinforcement distribution and clear interface was perceived in the micro structural and energy dispersive spectroscopy analysis of composite material. It was observed from XRD analysis that no secondary (intermetallic) phase of Al and ZnO were present in the composite material. The simultaneous thermal analysis of the composites was done to understand the variation in the exothermic peak temperature and weight change percentage of composite material. The developed composite material with 5wt.% ZnO exhibited promising

results in terms of micro-hardness (~2 times), nano hardness (~3.5 times) and elastic modulus (~1.9 times) greater value compared to Al. The increased addition of ZnO nanorods in aluminium shows enrichment in properties rendering the material suitable for different engineering applications.

Keywords: Composite material; Microwave hybrid sintering; Interfacial characteristics; Microhardness; Microscopy; Nano indentation; X-ray diffraction.

Zinc oxide nanorods effect in micro structural and mechanical characteristics of aluminium composite material

Abstract:

In the present study, aluminium zinc oxide (Al-ZnO) nanorods composites with 3.5 and 5 wt.% ZnO in Al were manufactured using powder metallurgy and microwave hybrid sintering. A fairly uniform reinforcement distribution and clear interface was perceived in the micro structural and energy dispersive spectroscopy analysis of composite material. It was observed from XRD analysis that no secondary (intermetallic) phase of Al and ZnO were present in the composite material. The simultaneous thermal analysis of the composites was done to understand the variation in the exothermic peak temperature and weight change percentage of composite material. The developed composite material with 5wt.% ZnO exhibited promising results in terms of micro-hardness (~2 times), nano hardness (~3.5 times) and elastic modulus (~1.9 times) greater value compared to Al. The increased addition of ZnO nanorods in aluminium shows enrichment in properties rendering the material suitable for different engineering applications.

Keywords: Composite material; Microwave hybrid sintering; Interfacial characteristics; Microhardness; Microscopy; Nano indentation; X-ray diffraction.

1. Introduction:

Aluminium metal matrix composite (Al-MMCs) exhibit higher strength to weight ratio, good corroion resistant properties, wear resistance and excellent modulus. Therfore, it is widely used in automobile, aerospace and military applications. For instance, Al and its alloy can replace mild steel (MS) and cast iron (CI) component (*i.e.* brake block, disc, pistons) to a greater extent by a reduction in weight and improving fuel efficiency [1–3]. However, lower strength, modulus and ductility of Al limit the wider application in the process industry. These

limitations can be greatly eliminated by use of alloying elements in the Al. In the recent years, numerous researchers has presented the various reinforcement in the form of particulate, short and long fibers to enhance the mechanical response of the material [4–8]. The various oxides (CeO_2, Al_2O_3, SiO_2, Y_2O_3, ZrO_2, ZnO), borides (TiB_2, ZrB_2), intermetallic component (Fe_3Al, Ni_3Al), carbides (SiC, TiC, TaC), nitrides (Si_3N_4, TiN) and other inorganic and organics (fly ash, carbon fibres, CNT, SWCNT, MWCNT) in Al matrix were incorporated to form aluminum metal matrix composite (Al-MMCs) with improved strength and ductility concurrently in the components to endure longer service life [9–13]. Samal et al [14] reported the effect the TiC content (5, 7 and 9 wt.%) on the AA5052 for mechanical properties. They observed that the formation of intermetallic (Al_3Ti) during synthesis process is prime factor for the improvement in the tensile (78% higher ultimate strength) and wear resistance (30% lower volume loss) of the composites with a compromise in impact strength (36% lower value). Similarly, Lanthanum (La) based oxide material was utilized by Chen et al [2] as reinforcing elements in Al6061 for different applications in aerospace, marine and military application. They observed 3.6 times higher hardness with 0.5 wt.% La and higher elastic modulus (2.89% higher) with uniform interfacial characteristic between the reinforcement and matrix. Subsequently, Singh et al [15] suggested that the higher sintering pressure is favourable for the improvement in the densification behaviour and material outcomes (*i.e.* hardness and elastic modulus) for Al-0.5wt.% MWCNT. The investigator suggested improved compressive (30% higher) and hardness (13% higher) when compaction pressure was increased to 80MPa from 30MPa during spark plasma sintering process. Recently the zinc oxide (ZnO) nano particles were reported for Magnesium (Mg) based composite material for excellent mechanical property enhancement. Tekumalla et al [16] confirmed 53.3% and 27% higher hardness and ultimate tensile strength with the addition of 2.5 wt.% ZnO in Mg-3Al-0.4Ce alloy material. Similar observations were

given by Chen et al [17] by introducing 2 wt.% ZnO nano particles in Mg-4Zn-3Gd-1Ca alloy the compressive strength (703.4 ± 39.8 MPa) improves drastically (*i.e.* higher than mild steel).

In our previous studies [18] the ZnO nanorods reinforced Al composite was successfully synthesised with two different (0.5 and 2wt.%) reinforcement amount. It has been observed that the presence of ZnO nanorods in the matrix improve the micro hardness and elastic modulus by ~28 and ~32% respectively for 2wt.% ZnO nanorods in Al. There is no adequate co-relation between the interfacial features and mechanical properties of material at the nano scale in the open literature or previous work done for Al-ZnO nanorods composite material [19–21]. As a result, it is intriguing to learn about the intermetallic components, interfacial properties, and mechanical behaviour of the synthesized composites. As a result, in the current study, Al composites with two distinct ZnO reinforcement contents (3.5 and 5wt.%) were created using a solid-state manufacturing process and a microwave hybrid sintering methodology. The primary goal of this research is to investigate material properties and determine the interfacial features, physical and mechanical response of the Al-ZnO composite material. To elucidate the secondary product (intermetallic) generation during the synthesis process, a phase transition study and simultaneous thermal analysis of the composite were performed.

2. Materials and methods

Aluminium (Al) with purity 99.75% used as matrix material and for reinforcing element (ZnO nanorods) zinc acetate (purity 99.75%) was utilized. The raw materials were procured from procured from Alpha Chemika Pvt. Ltd. Mumbai India. The synthesis of ZnO nanorods was done as per well-established thermal decomposition method. The comprehensive documentation on the formation of ZnO nanorods can be found in our previous research [18]. In the present work, two different reinforcement percentage (3.5 and 5 wt. %) was utilized for the fabrication of the composite material. The matrix (Al) and reinforcement (ZnO) were

subjected to mixing with the help of mechanical ball milling process. The milling was done with ball to powder ratio set at 10:1 with 150 rpm for 12 hours at ambient temperature and pressure. Simultaneous, thermal analysis (STA) of the composites were done using STA system (model: SDT Q600) for differential scanning calorimetry (DSC) and thermo-gravimetric analysis (TGA) under N_2 environment for maximum temperature of 700 °C. The homogeneously mixed powder material was cold compacted with compaction pressure of 580MPa. The green compacted part was sintered using well established innovative microwave hybrid sintering unit as per previous study [13,18]. The sintering temperature was kept 630±5 °C at ambient environment. The phase transformation study was done with the help of X-ray diffraction using Bruker D8 advanced (Cu-K_α; λ=1.5406Å) with scan speed of 1.5 degree/min. X-ray photoelectron spectroscopy (XPS, Make - Physical Electronics; Model- PHI 5000 VersaProbe III) was utilized for determination of valance state of elements. The surface morphology of the composite was assessed using scanning electron microscope (FESEM, ZEISS) equipped with energy dispersive spectroscopy (EDAX). For the interfacial characteristics of composite transmission electron microscopy (HRTEM with SAED; make: JEOL/JEM 2100) was utilized. The relative density of composite material is calculated using Archimedes principle. For the measurement of hardness, ASTM standard E384-99 was utilized and 100 gf with dwell time of 10 s. Mitutoyo HMV 200 automatic micro-hardness tester was used for the measurement of hardness. The depth-sensing mechanical behaviour was assessed with the help of Hysitron nano indentation apparatus. The maximum applied load during indentation behaviour assessment were taken as 2000 micro newton [15,22,23]. For the measurement of load displacement during indentation test Berkovich diamond tip was utilized. The schematic representation of the fabrication of composite material, hybrid microwave sintering process and macroscopic observation of the composite material can be seen in Fig. 1. The morphology of the as received Al and synthesised ZnO nanorods can be seen in Fig. 2.

The measured length observe through HRTEM analysis of the ZnO nanorods is in the range of 76 to 168 nm [18]. The XRD spectrum of as synthesized ZnO nanorods has been given in Fig 2(e). Standard ICDD diffraction data has been utilized for identification of matching peaks.

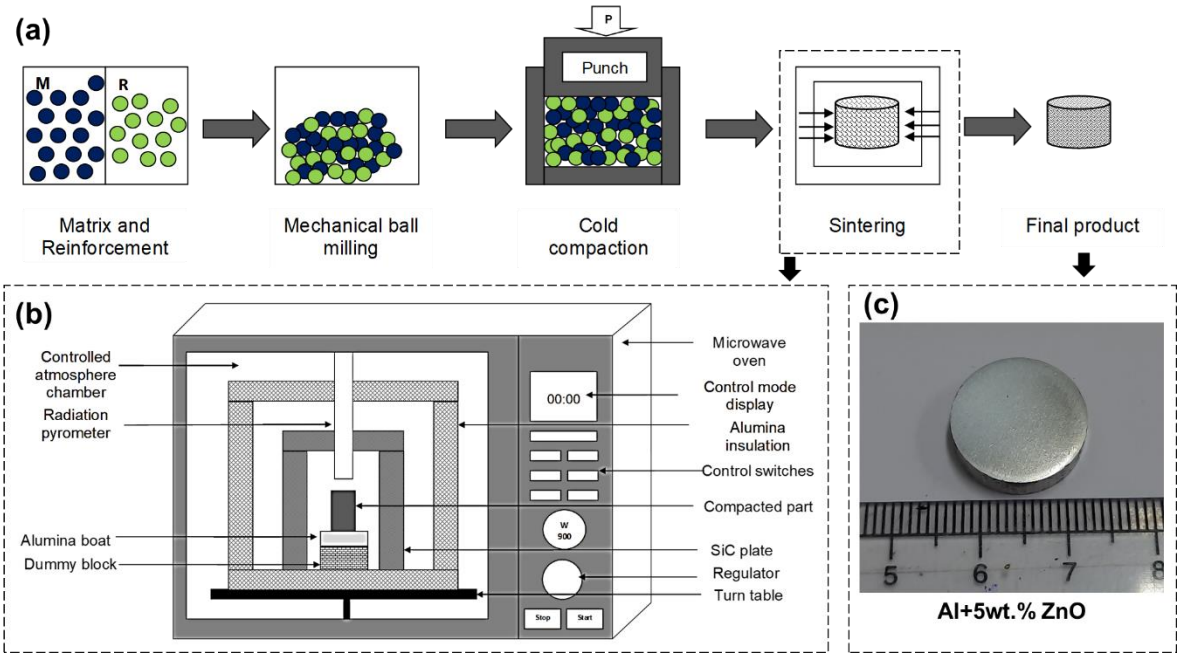

Fig. 1. (a) Schematic representation of the fabrication of composite material; (b) detailed sketch of hybrid microwave sintering process and (c) macrostructure view of hybrid microwave sintered composite material

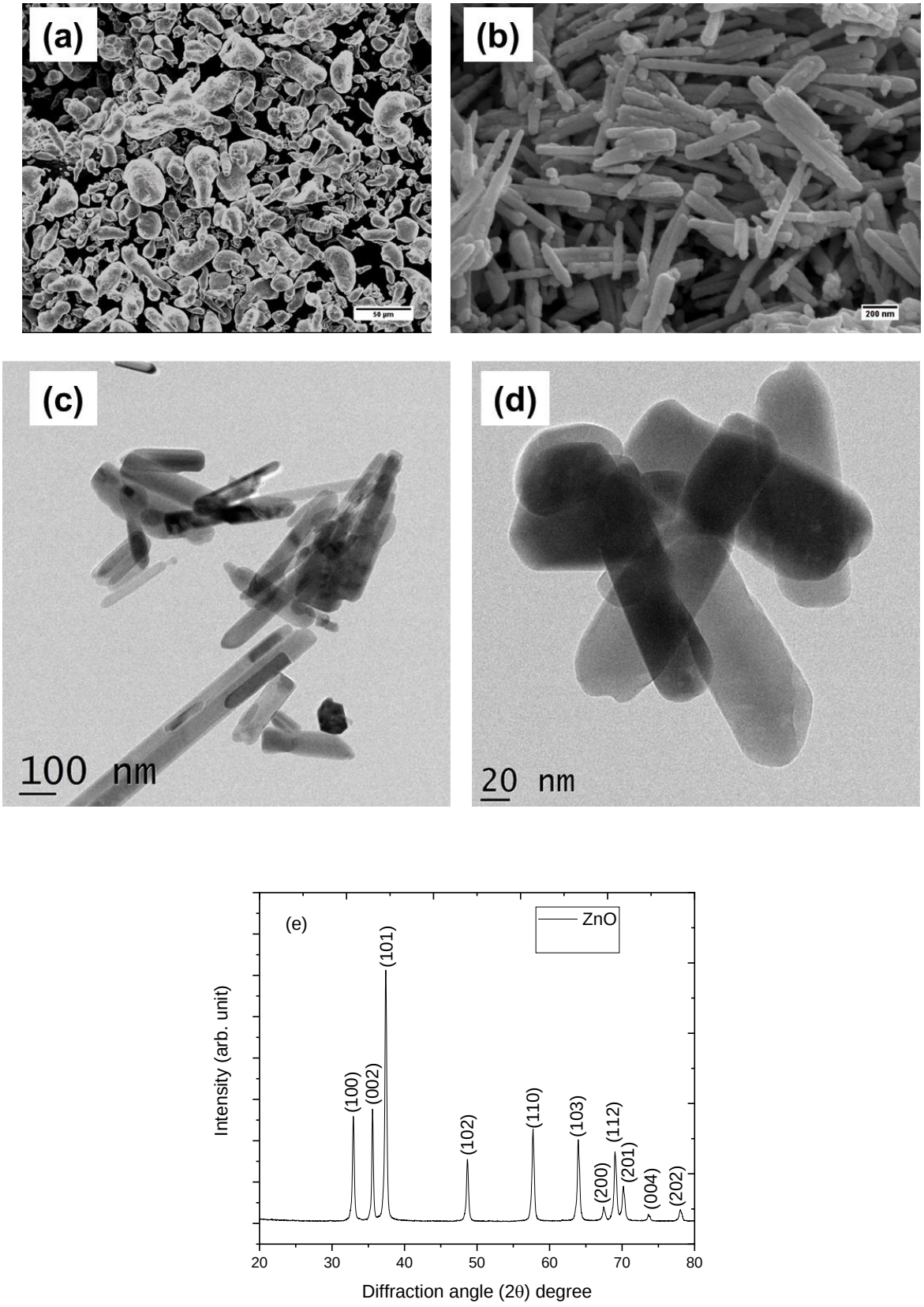

Fig. 2. As received aluminium powder (a), (b) FESEM image of ZnO nanorods (c) & (d) HRTEM image of ZnO nanorods (e) XRD spectrum of ZnO nanorods

3. Results and discussion

3.1. Synthesis of composites using microwave hybrid sintering

Aluminium and Al-ZnO composite material were successfully synthesized with powder metallurgy and microwave hybrid sintering process. The macroscopic observations (Fig. 1c) of the fabricated material reveal no surface cracks and radial defects. It may be noted that the conventional sintering of Al-MMCs requires more than 2 to 4 hour (including heating and holding period) while it only took 11 minutes to process in microwave in normal atmospheric medium. The green and sustainable synthesis microwave hybrid sintering process reduce the overall processing time with maximum of ~95% cycle time. The power consumption is significantly reduced ~85% compared to conventional sintering techniques for Al-MMCs under normal working environment [18,24].

3.2. Simultaneous thermal analysis of the composite material

The variation of weight change and derivative heat flow with temperature for Al and Al+5wt.% ZnO composite material can be seen in Fig. 3. The variation for the composite material weight change is considerably (~4%) lower compared to Al as observed from TGA graph. The reduction in the weight change of composite material is a strong function of reinforcement content. There are no significant changes in the onset, exit and endothermic peak of composite material was noticed. This shows the improve wettability and good bonding with the matrix material [18,25,26]. The observed variation is tabulated (Table 1) to extract the different temperature zone in Al and composite material. There are small variations (~1 °C lower) in onset temperature and ~2 °C higher value is noted for exit weight change and endothermic peak temperature in case of composite material compared to Al. The very small fraction of variation in the DSC curve can be justified by the complete diffusion of reinforcement and no secondary

intermetallic phase from Al and ZnO system. On a similar observation, below 900 °C no chemical reaction were noted for Al-ZnO composite material [25].

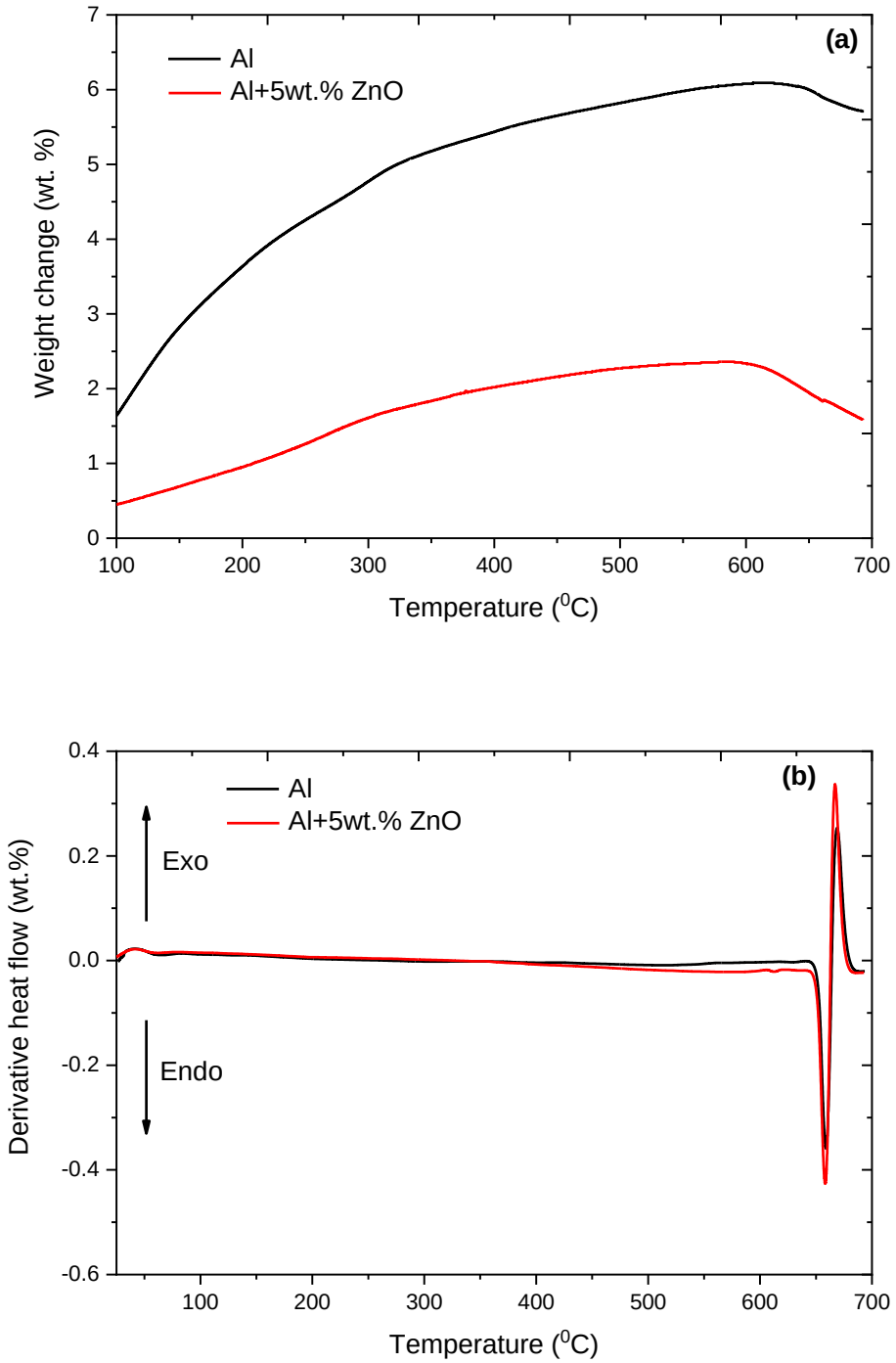

Fig. 3. (a)TGA and (b) DSC curve for the aluminium and Al+5wt.% ZnO composite material

Table 1: Temperature zone in the Al and composite material from DSC curve

Material	Onset rapid weight change temperature(°C)	Exit rapid weight change temperature(°C)	Peak temperature at endothermic point (°C)
Al	~651	~661	~657
Al+5wt.% ZnO	~650	~663	~659

3.3. Surface morphology and distribution mapping with EDAX

The surface morphology of the mechanically milled composite powder material after 12hrs is given in Fig.4a. The individual elemental mapping is of composite powder is shown in Fig.4b. The uniform distribution of the reinforcement is major concern in composite material fabrication. As non-homogenous distribution and large accumulation of reinforcement leads to unpredictable failure. The milling time and control over the processing medium defines the distribution and behaviour of composite material. In the present case a part of the reinforcement (ZnO nanorods) were seen to agglomerate with small cold welding with the matrix phase (Al). Normally, nano-particles and nanorods are having higher surface energy leads to formation of cluster and partial cold welding during milling process [2,27,28]. Similar observations were reported by Sankaranarayanan et al [29] for Mg-ZnO nano-composites (size of ZnO<200 nm). A very few part of the nano-particles seams to develop range of hundred nanometers cluster in the composites near the grain boundaries. Figure 5a represent the surface morphology of the microwave sintered Al+5wt.% ZnO composite material. A comparable observation were made by Bastwros et al [30] for uniform distribution of the graphene in Al6061 alloy material. Their observation suggest that milling have minimal influence on the reinforcement damage but helps

in homogeneous dispersion in the composite material. The uniform distribution effective diffusion is clearly visible on the surface of the composite material. To illustrate the presence of reinforcement elemental mapping and point EDAX is done (Fig. 5b). The distribution mapping resembles the uniform dispersion of ZnO nanorods in Al. The retention and effective diffusion of ZnO nanorods in composite displayed on the composite material. The reinforcement rich phase in composite material given in Fig. 5a by the EDAX spectrum 36 and 37 and corresponding elements were highlighted. The small amount of oxygen in the EDAX spectrum shows the integral phase of reinforcement. The reinforcement appears individually with minimal traces of cluster in sintered phase in composite material. Here, the compaction pressure and sintering temperature plays a significant role in final morphology of the composite material. It has been observed that increasing pressure and sintering temperature leads to uniform micro structure and reinforcement embedment with matrix phase [31,32].

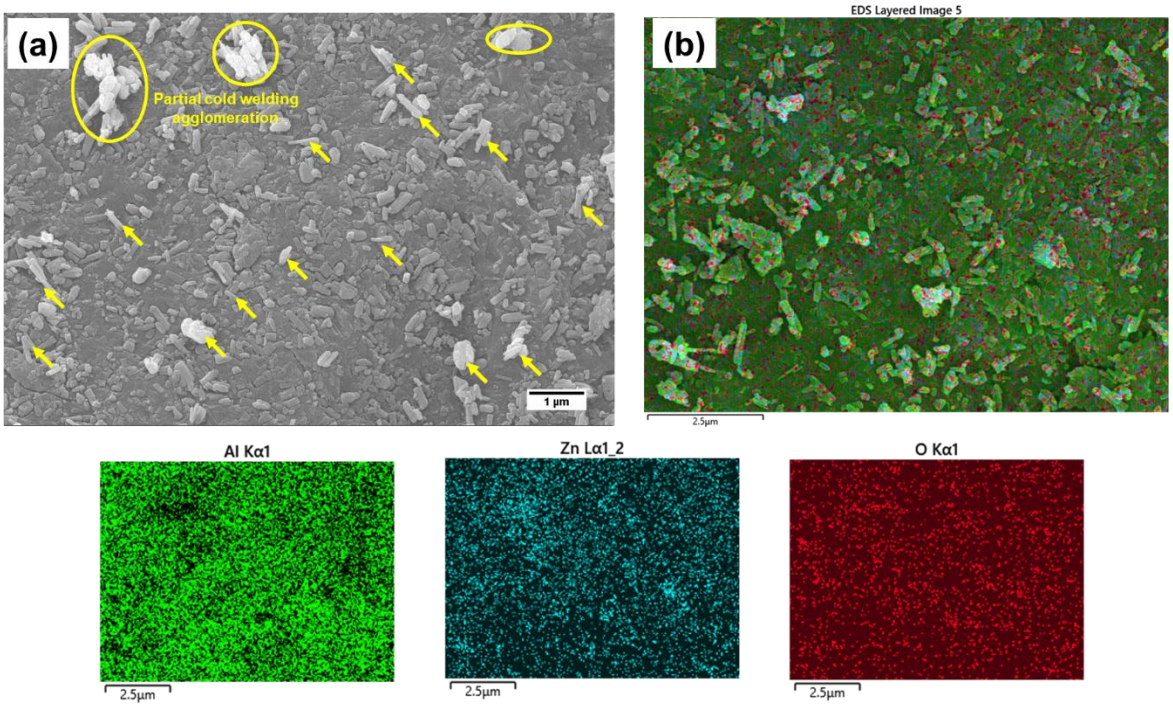

Fig. 4. (a) Scanning electron microscopy image of the Al+5wt.% ZnO composite after mechanical milling for 12hrs. (b) The particle distribution and mapping of the individual elements (matrix and reinforcement) are presented in different colour

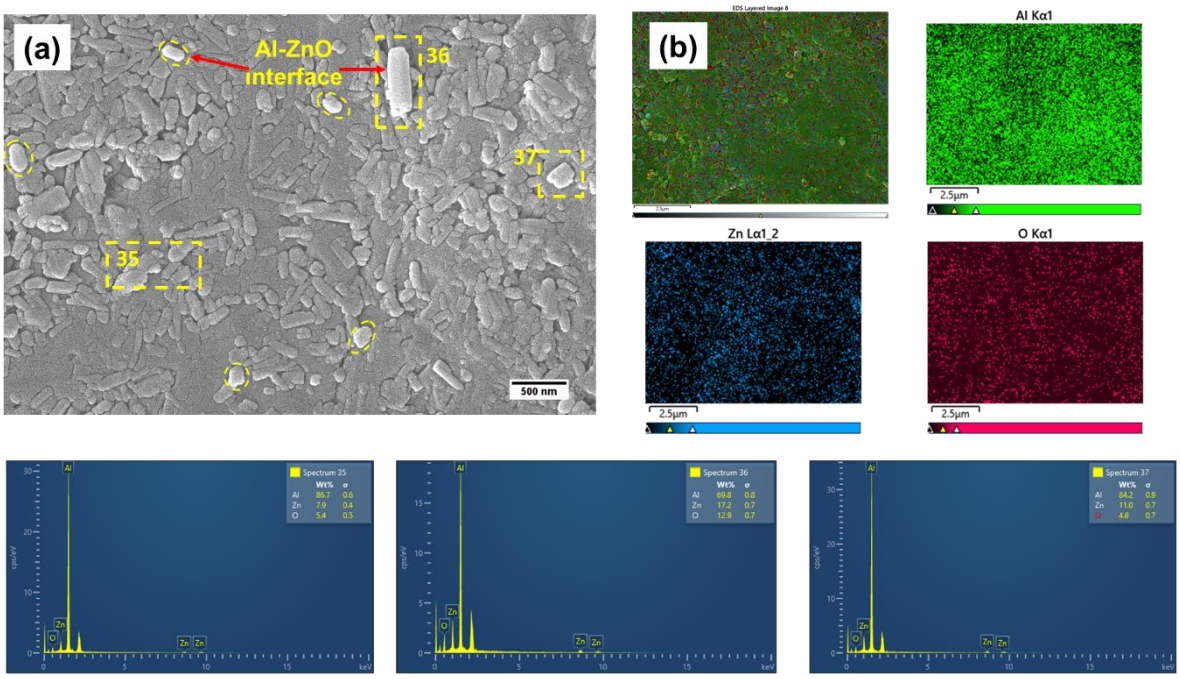

Fig. 5. (a) Surface of the microwave sintered Al+5wt.% ZnO composite. (b) The mapping of the individual element (Al, Zn and O) and point spectrum of the sintered surface for identification of the matrix and reinforced phase.

3.4. Interfacial characteristics of and phase transformation behaviour composites material

Figure 6 (a-d) depicts the transmission electron microscopy (TEM) image of Al+3.5wt.% ZnO composite material. Figure 6a depicts the uniform retention of reinforcement and matrix material with generation of nano crystalline phase in the composite. It is evident from Fig. 6 (b-d) that no cracks or dislocations line is visible in the interfacial zone of matrix and reinforcement. A uniform and clear interface is ensured by formation of strong diffusion bonding between the Al and ZnO nanorods. Moreover, the load bearing capacity of the

composite is increased by the formation of strong bonding and homogenous interface [15,31]. Similar observations was reported by Singh et al with minimal porosity and no interfacial product for Al/MWCNT composite material processed by spark plasma sintering method [15]. In this context Ao et al explored the effect of rare earth oxide (La_2O_3) addition on Al composite with TiC and Al_2O_3 ceramic particles and found no intermetallic phase. Their findings reveals that the addition of rare earth oxide enhances the wettability of the carbon in Al matrix which promoted for the formation TiC grain after reaching a critical concentration for interfacial product generation [33]. In this scenario, the reinforcement in the composite material has high physical integrity (Fig. 6 b, c & d). Figure 7(a & b) shows the XRD analysis of the Al and Al+5wt.% ZnO composite material. It is evident from Fig. 7b that for composite material most intense peak of Al corresponding to diffraction plane Al(111), Al(200), Al(220), Al(311) was observed with less intense peak of ZnO(100) and ZnO(110). All the peaks are indexed as per standard diffraction data (ICDD) [15,34]. The XRD data exhibit no secondary intermetallic phase from Al and ZnO. This process lead to the effective diffusion of reinforcement with matrix material. The results obtained from XRD are in good agreement with the SEM and TEM analysis of the composite material. Similar observation were reported by Rashad et al [35] for graphene nanoplatelets (GNPs) reinforcement in Al. No secondary intermetallic phase or extra peak were noticed for Al/0.3 wt% GNPs composite material. Bastwros et al [30] also described the unaffected XRD pattern with the addition of graphene on Al6061 alloy material. This fact can be attributed to sensitivity of the XRD equipment and very low level of reinforcement. However, the distinct phase of reinforcement and matrix can be clear seen from the micro structural characteristics of the composite material. Further work in the direction of the phase transformation and interface behaviour are continuing.

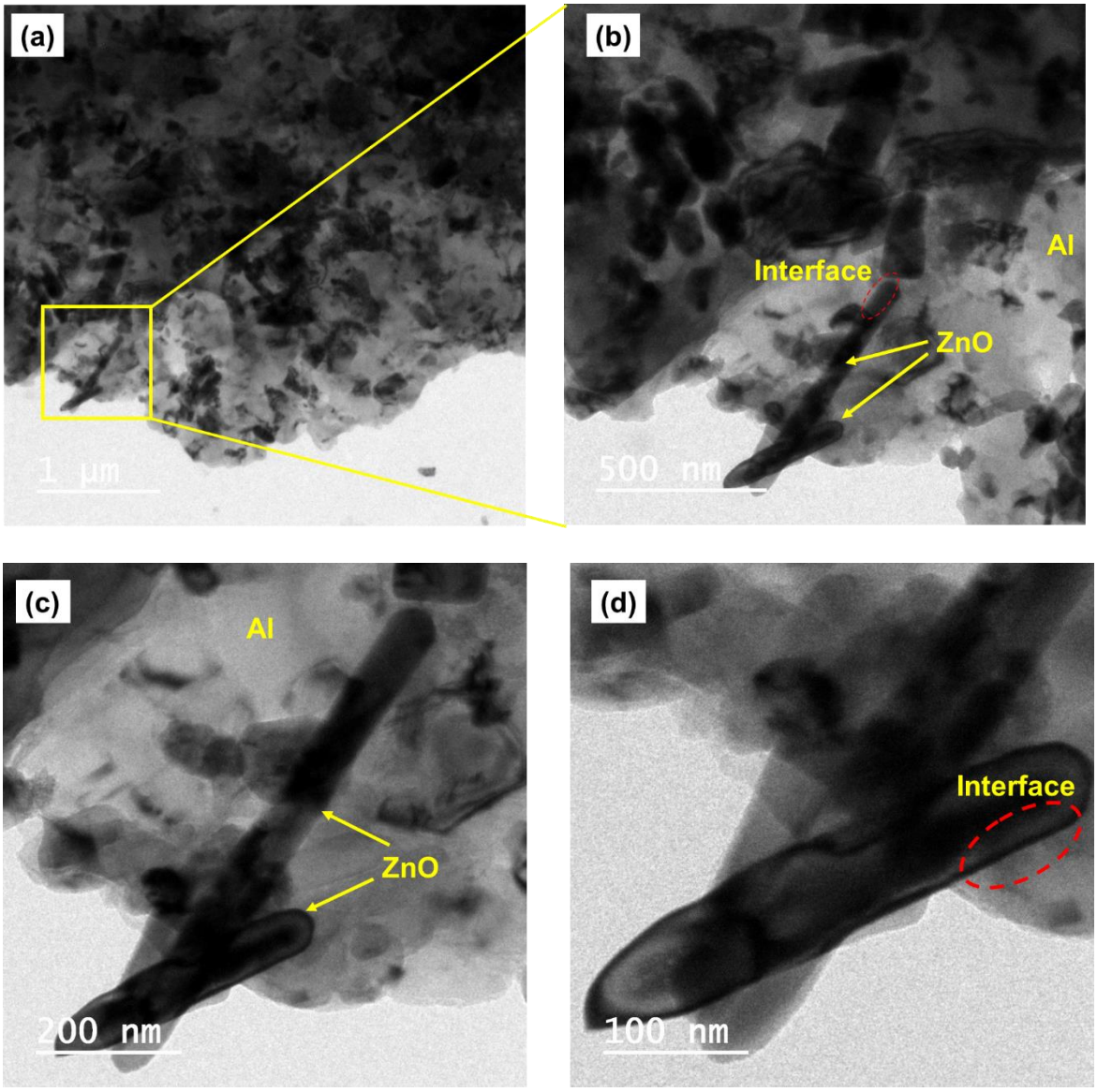

Fig. 6. Transmission electron microscopy (TEM) image of the Al+3.5ZnO composite material (a) low magnification image (b, c & d) different magnification image of Al+3.5ZnO composite material of showing the interface line between Al and ZnO and distribution of nanorods in the matrix material.

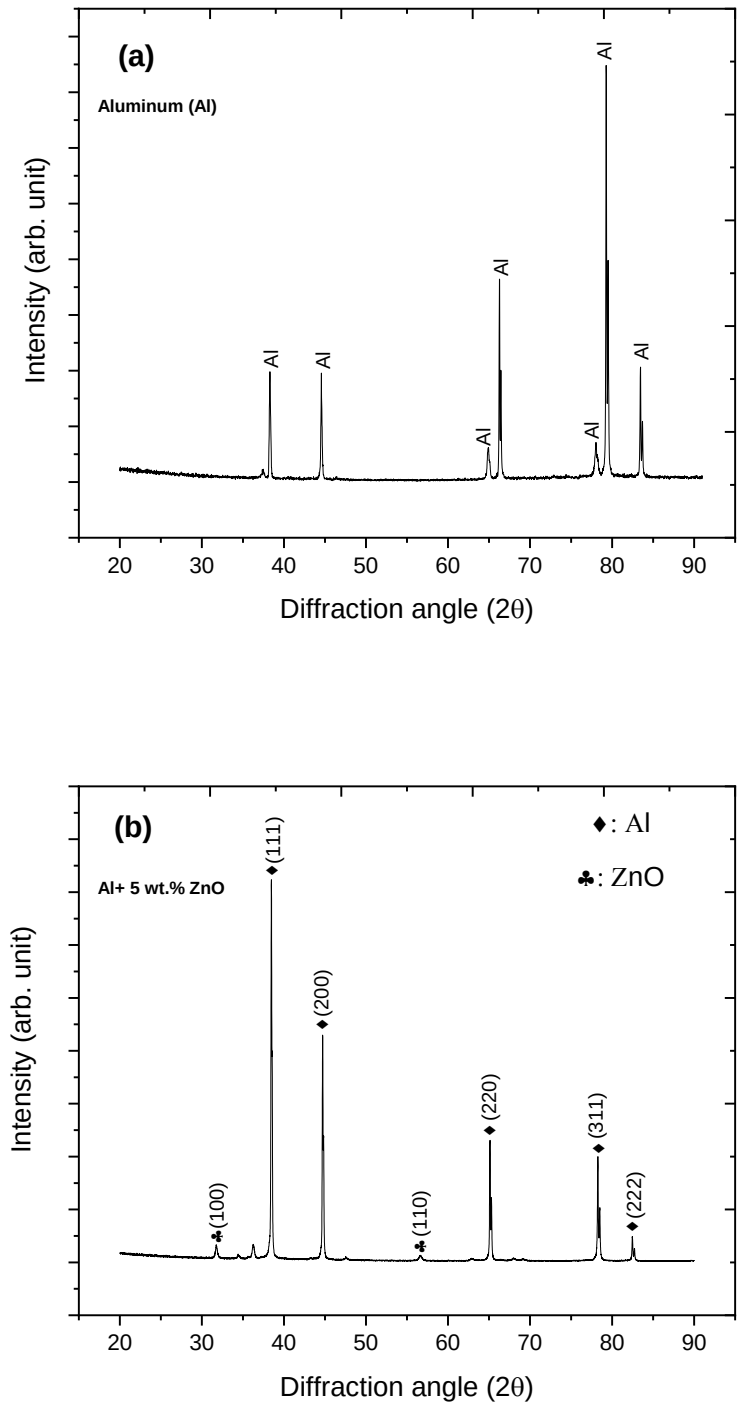

Fig. 7. X-ray diffraction pattern of hybrid microwave sintered (a) Al and (b) Al+5wt.% ZnO composite material

3.5. XPS study of composite material

XPS spectroscopy was used to determine the elemental composition Al and composite material. The XPS spectra of Al and Al-5wt.% composite material revealed the typical peaks of various elements (Fig. 8a). The XPS examination revealed that the primary elements in the composite material were C, Zn, O, and Al, with no impurities. The carbon contamination is seen in the XPS spectra of C1s (Fig. 8b), which serve as a reference point for binding energy measurements at 284.6 eV. Figure 8c shows the XPS spectrum of Al 2p at 74.2 eV having good symmetry. From the Zn 2p XPS spectra (Fig. 8d), the divalent oxidation states Zn 2p1/2 and Zn 2p3/2 were seen with binding energies of 1044.72 eV and 1021.67 eV, respectively. The modest variation (~1 eV) in the binding energy of Al 2p exhibit the formation of bonding between the Al-Zn and Al-O during addition of ZnO nanorods in monolithic phase. The appearance of Zn peak in composite material indicate the successful diffusion into the Al lattice and an Al-O bond has been formed at interface region of ZnO [36,37]. Oxygen atoms in ZnO nanorods reinforcement phase, which are features of O^{2-} ions on the wurtizite structure of a hexagonal Zn^{2+} ion array, were attributed to the presence of oxygen on composite material with binding energy 531.07 eV (Fig. 8e). Similar observation was given for the Al doped ZnO nanorod in the surface of Si substrate material by Yun et al [37] for binding energy of different elements. According to the XPS results, ZnO nanorods do not react or form any intermetallic and successfully diffuse into the unoccupied site of the Al matrix, which is favourable to improving the interfacial bonding in Al-5wt.% composite material.

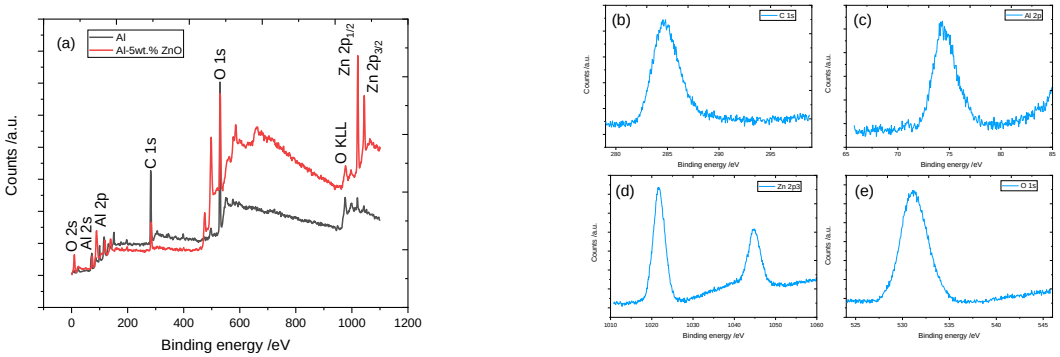

Fig. 8. X-ray photoelectron spectroscopy (XPS) analysis of (a) microwave hybrid sintered Al and Al-5wt.% ZnO composite material and wide scan XPS spectra of Al-5wt.% ZnO composite material (b) C 1s spectra, (c) Al 2p spectra, (d) Zn 2p3 spectra, (e) O 1s spectra

3.6. Relative density and Micro-Hardness of the composite material

Figure 9 illustrate the variation in the relative density and micro-hardness value of the Al and composite material. It is evident from Fig. 9 that higher amount of ZnO content in Al slightly reduces the relative density. The slight reduction in relative density may be attributed to compaction pressure and higher amount of reinforcement phase. This is due to higher amount, small bunching of ZnO nanorods in composite material and limitation of conventional compaction in powder metallurgy process. However, the micro hardness value of the composite material is in increasing trends with reinforced phase. The micro hardness value is ~111% improvement is observed for 5 wt.% ZnO nanorods composite material. This higher amount of hardness is attributed to the higher deformation resistance of the material in presence of hard and stiff reinforcement phase. Also, the enhanced surface resistance can be described due to presence of nano ZnO phase in the Al [18,19]. The improved interface and well bonded matrix and reinforcement is prime reason for the higher hardness in composite material. Moreover, the hybrid microwave sintering technique helps in achieving uniform near dense micro structure and higher hardness compared to conventionally sintered materials [34,38]. On a

similar note Tekumall et al reported ~53% higher micro-hardness value for Mg-3Al-0.4Ce alloy using ZnO nano particles [16]. Samal et al stated an increase in 32% higher hardness due to formation of Al_3Ti intermetallic phase in AA5052 material [14].

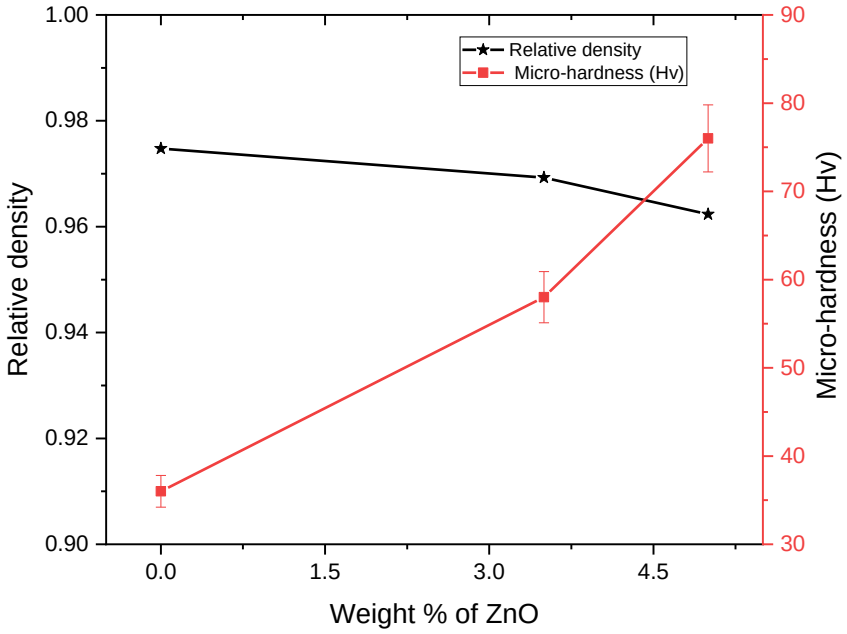

Fig. 9. Variation of the relative density and micro-hardness value for the aluminum and composite material as a function of ZnO amount

3.6. Depth sensing Indentation Response of the composite material

Figure 10a depicts the variation in the load displacement graph for Al and composite material. It is evident from the Fig. 10a that for composite material with 5 wt.% ZnO nanorods the indentation depth is minimum. This resembles the hindrance of the indenter movement to higher depth due to presence of hard ceramic phase [2,15]. The uniform dispersion of ZnO nanorods results in composite material with significantly higher nano hardness and elastic modulus. In the current work the highest value of nano hardness (2.0110 GPa) and elastic modulus (108.4573 GPa) is achieved with 5 wt.% of ZnO nanorods in composite material. The

variation in the nano-hardness and elastic modulus value of Al and composite material is given in the Fig.10 (b & c) The following key point can be given to explain the higher value of nano hardness and elastic modulus response for composite material:

- The mismatch in the thermal expansion co-efficient of the aluminium and ZnO. Heating the composite material near the melting point of the matrix material in microwave hybrid sintering generate the necessary dislocations due to large variation in the CTE value of Al (21 X 10^{-6} K^{-1}) and ZnO (29 X 10^{-7} K^{-1}). Also the mismatch in the elastic modulus value of the Al and ZnO and presence of ZnO nanorods in increasing amount increase the dislocation density.
- Strengthening due to presence of nano metric level ZnO in the composite material as per effectively Hall-Petch relation.
- Dispersion strengthening due to uniform distribution of the reinforcement phase in composite material.
- Uniform and clear interface and absence of any impurities during synthesis process lead to higher densification and improved mechanical properties.

A pictorial representation of the load applications and reinforcement distribution is given in Fig. 11 The randomly oriented reinforced phase will have higher strength and less tendency toward to failure to obstruction of grain during operating zone [27]. In case of parallel and perpendicular orientation of the distributed ceramic phase the matrix and reinforcement is weekly bonded and propagation of crack will be higher due to less energy requirement to fracture. However, randomly oriented reinforced phase in composite materials leads to the strong interlinking between matrix and reinforcement [2,16]. Further this fact is more apprehended by the work hardening behaviour of the composite material. The work hardening behaviour of the material is defined as the resistance to deformation under the application of load. The value of work hardening for the composite material is given in the Table 2. It is

marked that the higher resistance is offered by the 5 wt.% ZnO nanorods composite material compared to Al. The higher value of the H^3/E_r^2 relates to the better wear resistance of the material [2,23]. In the current work ~14 times higher amount of surface resistance is observed compared to Al for 5 wt.% ZnO nanorods composite material. Further research in this area is being conducted to better understand the responses of composite materials under various sorts of loading conditions. In this investigation, a comparison of the mechanical behaviour of created material yields better findings than in the previous one (Table 3). Microwave hybrid sintering has been shown to be effective in achieving good mechanical response in Al-MMCs. The fabricated material can be used in automotive (suspension link, piston material, brake drum, etc.) and aerospace (landing gear component) for different components with higher specific strength and good wear resistance properties. The current study's findings allow us to recommend a zinc oxide nanorod-based aluminium composite material with high hardness and elastic modulus compared to that reported in literature (Fig. 12 and 13). We think that the current work's effective synthesis of Al-ZnO nanorod composite material with microwave hybrid sintering can provide a big possibility to change the composite material strength with higher material responsiveness.

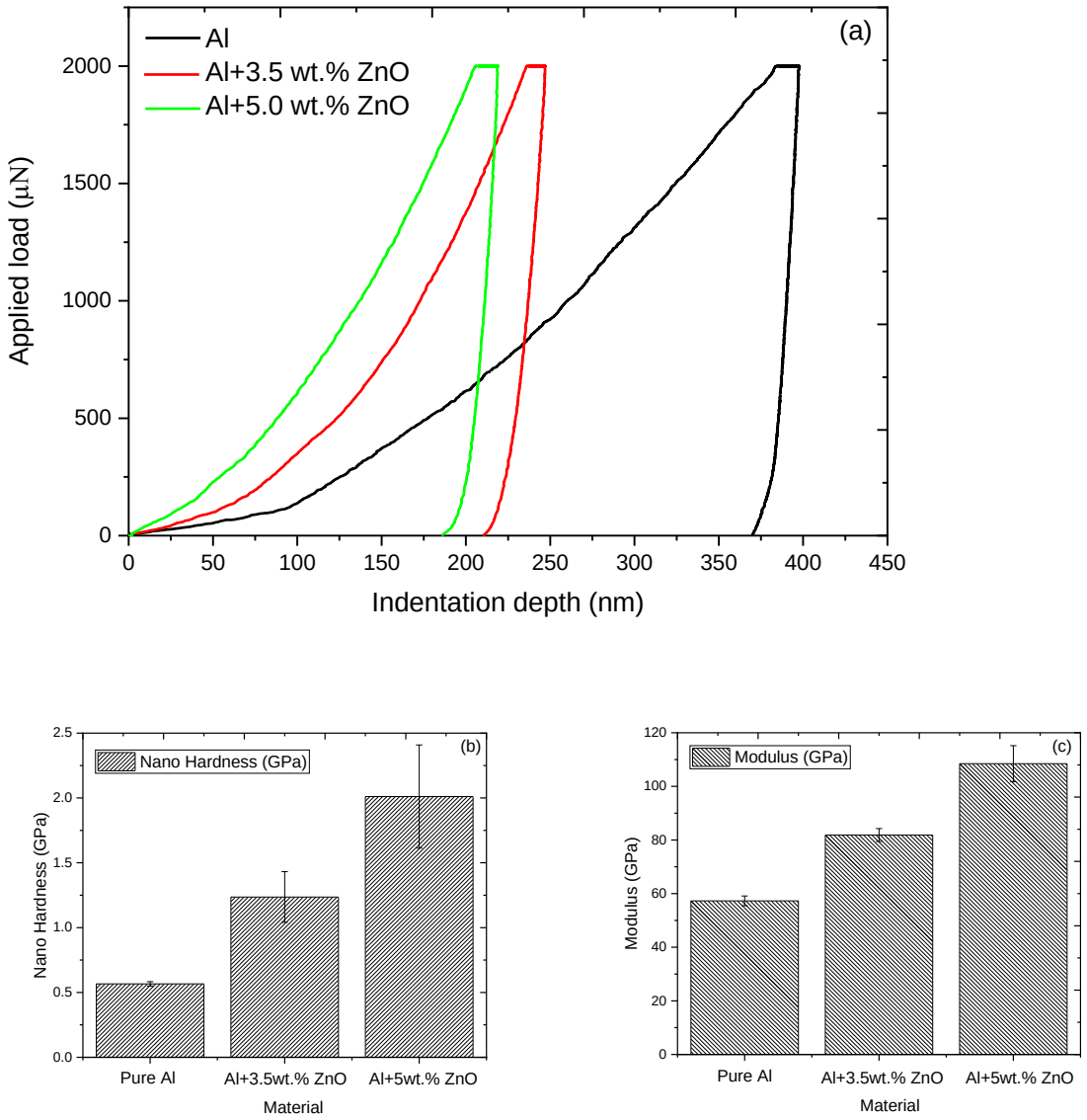

Fig. 10. (a) Variation in the load displacement graph; (b) nano-hardness and (c) elastic modulus for Al and composite materials

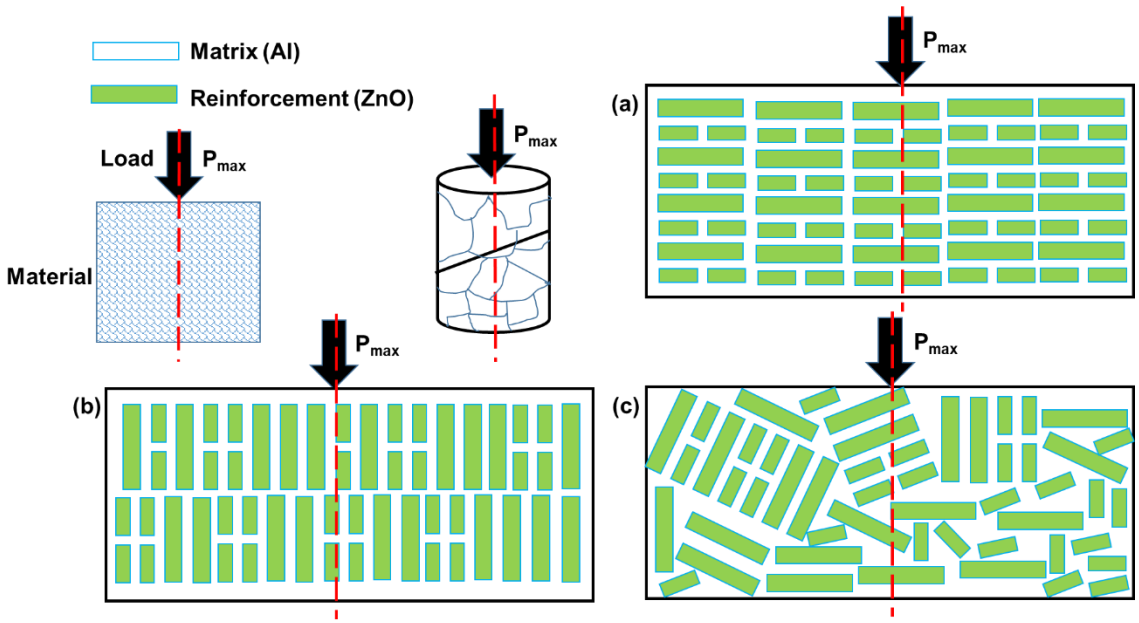

Fig. 11. Schematic illustration of the ZnO nanorods reinforcement distribution and role of alignment in the composite material on mechanical loading (a) reinforcement axis is perpendicular to load, (b) reinforcement axis is parallel to load, and (c) randomly aligned reinforcement in the composite material

Table 2. Value of the nano hardness, elastic modulus and plasticity index for the developed composite material.

Material	Nano hardness (GPa)	Reduced elastic modulus (GPa)	Plasticity index	
			(H/E_r)	(H^3/E_r^2) (MPa)
Al	0.5644	60.8865	0.009269	0.04853
Al +3.5wt.% ZnO	1.2360	85.0314	0.014535	0.26112
Al+5.0 wt.% ZnO	2.0110	110.0228	0.018278	0. 67184

Table 3: Matrix, reinforcing element, processing circumstance, hardness and elastic modulus data from the literature

Matrix	Reinforcing element	Reinforcement amount	Processing method and environment	Processing temperature and time	Hardness (Hv)	Elastic modulus E (GPa)	Ref.
Al	ZnO nano rods	0	Microwave hybrid sintering at atmospheric	630 °C for 11 minute	36	57.301	Current work
		3.5 wt.%			58	81.8463	
		5 wt.%			76	108.4573	
Al	GO	0	Conventional sintering at argon atmosphere	600 °C for 240 minute	~32.5	NR	Dasari et al 2018 [24]
		0.05 wt.%			~33		
		0.1 wt.%			~35		
		0.2 wt.%			~36		
Al6061	La	0.5 wt.%	hydrogen-argon atmosphere at	600 °C for 120 minute	88.5	83	Chen and Lin 2019 [2]
		1.2 wt.%			88.4	85.4	
		2 wt.%			55.9	53.3	
Al	$Cu_{50}Ti_{50}$	0	Microwave Sintering	600 °C for 240 minute	~40	NR	Reddy et al 2018[28]
		5 wt.%			~48		
		10 wt.%			~64		
		15 wt.%			~91		
Al6063	-	0	Conventional sintering	500-600 °C for soaking time of 60, 120 and 180 minute	41	NR	Ahamed, and Senthilkumar 2011 [39]
	Al_2O_3	1.5 wt.%			46		
	Y_2O_3	1.5 wt.%			44		
	Al_2O_3 &Y_2O_3	0.75 wt.%			44		
Al	MWCNT	0.5 wt.%	Spark plasma sintered at 30MPa	500 °C	69±9.2	76±10.7	Singh et al [15]
			Spark plasma sintered at 50MPa		73±7.4	81±9.0	
			Spark plasma sintered at 80MPa		77±6.1	86±7.4	
Al	Al_2O_3	0	Microwave sintering	550 °C	37±3	73±5	Reddy et al [40]
		5 vol.%			52±5	77±6	
		10 vol.%			73±6	82±2	
		15 vol.%			92±5	88±9	
Al	-		compacting at high pressure and temperature (175 MPa and 550 °C)		34	71.7	Niste et al [41]
	IF-WS_2	20 wt.%			39	49.6	
	2H-WS_2	20 wt.%			45	50.1	
Al	BN	0	Microwave sintering	550 °C	37±3	71.65±0.02	Reddy et al 2018 [42]
		0.5 vol.%			48±4	71.88±0	

		1 vol.%			67±3	72.7±0.006	
		1.5 vol.%			88±4	73.08±0.017	
Al	rGO	0	Conventional sintering	550 °C for 120	26±1.3	NR	Liu et al 2016 [43]
		0.07			29±1.9		
		0.15			30.2±2.0		
		0.3			34.5±3.7		
Al	Si_3N_4	0	Microwave sintering followed hot extrusion	550 °C	37±3	73±5	Matli et al 2017 [44]
		0.5 vol.%			58±4	77±4	
		1 vol.%			72±3	83±4	
		1.5 vol.%			101±5	88±2	
Al	NiO	0	Stir casting at 850 °C		20.5±0.6	NR	Najarian et al [26]
		1 wt.%			23.7±1.8		
		2 wt.%			27.6±2.8		
		3 wt.%			34.8±2.9		
		4 wt.%			38.3±2.5		
		5 wt.%			41.7±3.3		

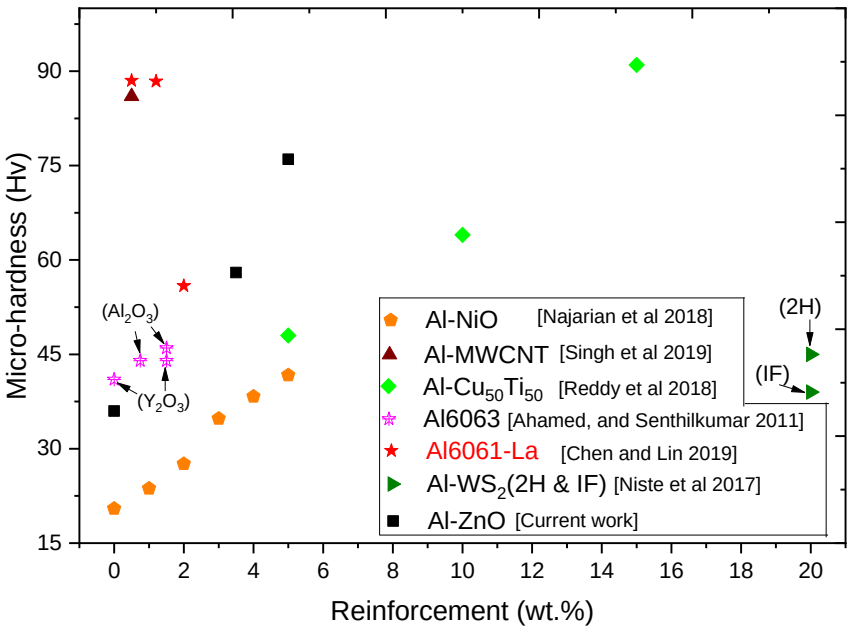

Fig. 12. Micro-hardness vs. reinforcement wt.% plot for different Al based composite material reported in literature

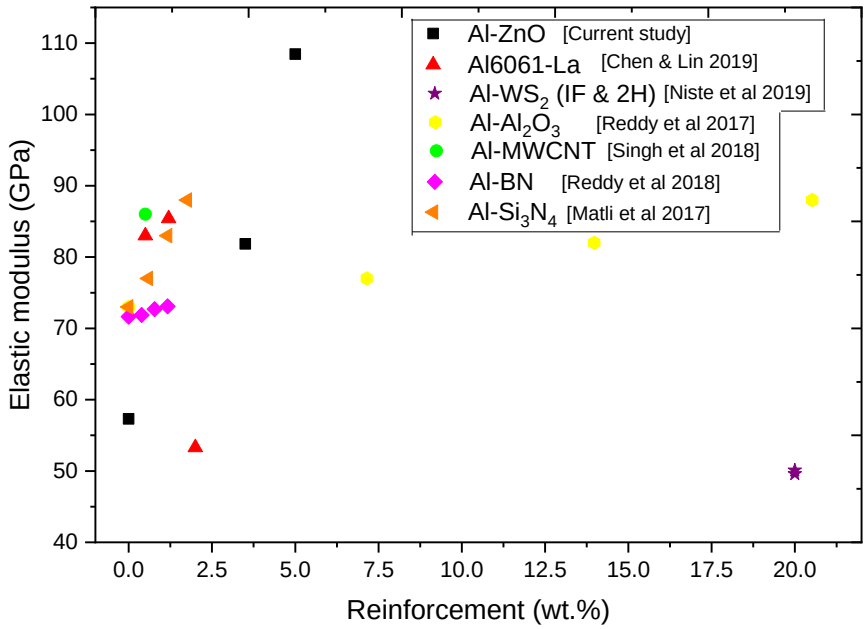

Fig. 13. Elastic modulus vs. reinforcement wt.% plot for different Al based composite material reported in literature

4. Conclusion

In the current work the role of ZnO nanorods in the mechanical and micro structural properties were calculated. The following conclusions can be given for the Al-ZnO composite materials:

- The aluminium and ZnO nanorods composite material is successfully synthesized by utilizing powder metallurgy and hybrid microwave sintering approach in normal atmospheric medium.
- The microwave sintered aluminium and Al-ZnO composite material shows nearly dense microstructure is possible to achieve with relative density of 0.9774.
- Appreciably uniform microstructure and clear interface is observed during the FESEM and HRTEM analysis of the composite material. From the EDAX analysis and point

mapping of the composite material exhibit smooth distribution of ZnO in the composite material.

- Significant improvement in the micro-hardness value was observed compared to aluminium. The maximum achieved micro hardness value is ~111% higher in case of 5wt% ZnO and ~61% higher in case of 3.5 wt.% ZnO nanorods in Al. Similar observations were noted for nano hardness value with a maximum of ~3.5 times higher value for 5 wt.% ZnO composite material.
- The excellent enhancement ~1.4 times and ~1.9 times higher elastic modulus were detected for 3.5 and 5 wt.% ZnO nanorods composite material respectively.

More research in the field of surface and wear resistance property assessment may be conducted to learn more about the function of ZnO nanorods reinforcement in Al. Changing the compaction pressure, sintering medium, inert environment, and harsh operating conditions may all be used to determine the ideal process parameters for achieving great repeatability on different attributes.

Acknowledgments

The author(s) would like to acknowledge Material Processing Research Laboratory of PDPM IIITDM Jabalpur for the fabrication and characterizations of the material. The financial support of this work received by IIITDMJ/ODRSPC/2017/2 and DST/SRG/2019/000571 is highly acknowledged. The support received from the nano indentation testing facility IIT Ropar and HRTEM analysis rendered by STIC SAIF Kochi is highly appreciated and acknowledged.

Data Availability

The authors confirm that the data supporting the findings of this study are available within the article.

Conflict of Interest

The authors declare that they have no known competing financial interests or personal relationships that could have appeared to influence the work reported in this paper.

Consent to Participate

Not Applicable.

Consent for Publication

All the authors have approved the final manuscript before submission.

References

[1] A. Taub, E. De Moor, A. Luo, D.K. Matlock, J.G. Speer, U. Vaidya, Materials for Automotive Lightweighting, Annu. Rev. Mater. Res. 49 (2019) 327–359. https://doi.org/10.1146/annurev-matsci-070218-010134.

[2] C.L. Chen, C.H. Lin, In-situ dispersed La oxides of Al6061 composites by mechanical alloying, J. Alloys Compd. 775 (2019) 1156–1163. https://doi.org/10.1016/j.jallcom.2018.10.093.

[3] S.K. Pattnaik, N.K. Bhoi, S. Padhi, S.K. Sarangi, Dry machining of aluminum for proper selection of cutting tool: tool performance and tool wear, Int. J. Adv. Manuf. Technol. 98 (2018) 55–65. https://doi.org/10.1007/s00170-017-0307-0.

[4] N.K. Bhoi, H. Singh, S. Pratap, Developments in the aluminum metal matrix composites reinforced by micro / nano particles – A review, J. Compos. Mater. 54 (2020) 813–833. https://doi.org/10.1177/0021998319865307.

[5] H. Singh, P.K. Jain, N. Bhoi, S. Pratap, Experimental study pertaining to microwave sintering (MWS) of Al-Metal Matrix Composite - A review, Mater. Sci. Forum. 928 (2018) 150–155. https://doi.org/10.4028/www.scientific.net/MSF.928.150.

[6] A. Sanaty-Zadeh, Comparison between current models for the strength of particulate-reinforced metal matrix nanocomposites with emphasis on consideration of Hall-Petch effect, Mater. Sci. Eng. A. 531 (2012) 112–118. https://doi.org/10.1016/j.msea.2011.10.043.

[7] N.K. Bhoi, H. Singh, P. Saurabh, Promise of Self-lubricating Aluminum-Based Composite Material, in: C. Prakash, S. Singh, J.P. Davim (Eds.), Funct. Smart Mater., CRC Press Taylor & Francis Group, 2020: pp. 65–82.

[8] N.K. Bhoi, H. Singh, S. Pratap, P.K. Jain, Microwave material processing : a clean , green , and sustainable approach, in: K. Kumar, D. Zindani, P. Davim (Eds.), Sustain. Eng. Prod. Manuf. Technol., 1st ed., Academic Press Elsevier, 2019: pp. 3–23. https://doi.org/10.1016/B978-0-12-816564-5.00001-3.

[9] R. Pérez-Bustamante, C.D. Gómez-Esparza, I. Estrada-Guel, M. Miki-Yoshida, L. Licea-Jiménez, S.A. Pérez-García, R. Martínez-Sánchez, Microstructural and mechanical characterization of Al-MWCNT composites produced by mechanical milling, Mater. Sci. Eng. A. 502 (2009) 159–163. https://doi.org/10.1016/j.msea.2008.10.047.

[10] M. Azadi, M. Zolfaghari, S. Rezanezhad, M. Azadi, Effects of SiO2 nano-particles on tribological and mechanical properties of aluminum matrix composites by different dispersion methods, Appl. Phys. A Mater. Sci. Process. 124 (2018) 1–13. https://doi.org/10.1007/s00339-018-1797-9.

[11] L. Kumar, S. Nasimul Alam, S. Kumar Sahoo, Influence of nanostructured Al on the mechanical properties and sliding wear behavior of Al-MWCNT composites, Mater. Sci. Eng. B Solid-State Mater. Adv. Technol. 269 (2021). https://doi.org/10.1016/j.mseb.2021.115162.

[12] P. Madhukar, N. Selvaraj, G.B. Veeresh Kumar, C.S.P. Rao, F. Mohammad, M. Chavali,

Effect of TiCnp on microstructure and mechanical behaviour of high-performance Al7150-TiC nanocomposites, Mater. Sci. Eng. B Solid-State Mater. Adv. Technol. 265 (2021). https://doi.org/10.1016/j.mseb.2020.115034.

[13] N.K. Bhoi, H. Singh, S. Pratap, M. Gupta, P.K. Jain, Investigation on the combined effect of ZnO nanorods and Y2O3 nanoparticles on the microstructural and mechanical response of aluminium, Adv. Compos. Mater. (2021) 1–22. https://doi.org/10.1080/09243046.2021.1993555.

[14] P.R. Samal, P.R. Vundavilli, A. Meher, M.M. Mahapatra, Influence of TiC on dry sliding wear and mechanical properties of in situ synthesized AA5052 metal matrix composites, J. Compos. Mater. 53 (2019) 4323–4336. https://doi.org/10.1177/0021998319857124.

[15] S.L. K, B. Alok, O. Akash, L. Tapas, Spark plasma sintered Al-0.5 wt% MWCNT nanocompoiste: Effect of sintering pressure on the densification behaviour and multi scale mechanical properties, Diam. Relat. Mater. 91 (2019) 144–155. https://doi.org/.1037//0033-2909.I26.1.78.

[16] S. Tekumalla, N. Farhan, T.S. Srivatsan, M. Gupta, Nano-ZnO particles' effect in improving the mechanical response of Mg-3Al-0.4Ce alloy, Metals (Basel). 6 (2016) 1–11. https://doi.org/10.3390/met6110276.

[17] Y. Chen, S. Tekumalla, Y.B. Guo, M. Gupta, Introducing Mg-4Zn-3Gd-1Ca/ZnO nanocomposite with compressive strengths matching/exceeding that of mild steel, Sci. Rep. 6 (2016) 8–12. https://doi.org/10.1038/srep32395.

[18] N.K. Bhoi, H. Singh, S. Pratap, Synthesis and characterization of zinc oxide reinforced aluminum metal matrix composite produced by microwave sintering, J. Compos. Mater. 54 (2020) 3625–3636. https://doi.org/10.1177/0021998320918646.

[19] C.L. Li, Q.S. Mei, J.Y. Li, F. Chen, Y. Ma, X.M. Mei, Hall-Petch relations and

strengthening of Al-ZnO composites in view of grain size relative to interparticle spacing, Scr. Mater. 153 (2018) 27–30. https://doi.org/10.1016/j.scriptamat.2018.04.042.

[20] Z. Guo, J. Xiong, M. Yang, W. Li, Microstructure and properties of tetrapod-like ZnO whiskers reinforced Al matrix composite, J. Alloys Compd. 461 (2008) 342–345. https://doi.org/10.1016/j.jallcom.2007.06.099.

[21] H.Y. Yue, W.D. Fei, L.D. Wang, Effects of heat-treatment on interfacial microstructures and tensile properties of ZnAl2O4 and ZnO coated Al18B4O33w/Al composites, Mater. Sci. Eng. A. 472 (2008) 231–234. https://doi.org/10.1016/j.msea.2007.03.066.

[22] W.C. Oliver, G.M. Pharr, An improved technique for determining hardness and elastic modulus using load and displacement sensing indentation experiments experiments, J. Mater. Res. 7 (1992) 1564–1583.

[23] J. Eckert, M.S. Dargusch, I.V. Okulov, S. Ehtemam-Haghighi, H. Attar, A.S. Volegov, D. Kent, M. Calin, H. Wendrock, M. Bönisch, Nanoindentation and wear properties of Ti and Ti-TiB composite materials produced by selective laser melting, Mater. Sci. Eng. A. 688 (2017) 20–26. https://doi.org/10.1016/j.msea.2017.01.096.

[24] B.L. Dasari, M. Morshed, J.M. Nouri, D. Brabazon, S. Naher, Mechanical properties of graphene oxide reinforced aluminium matrix composites, Compos. Part B Eng. 145 (2018) 136–144. https://doi.org/10.1016/j.compositesb.2018.03.022.

[25] T.G. Durai, K. Das, S. Das, Synthesis and characterization of Al matrix composites reinforced by in situ alumina particulates, Mater. Sci. Eng. A. 445–446 (2007) 100–105. https://doi.org/10.1016/j.msea.2006.09.018.

[26] A.R. Najarian, R. Emadi, M. Hamzeh, Fabrication of as-cast Al matrix composite reinforced by Al2O3/Al3Ni hybrid particles via in-situ reaction and evaluation of its mechanical properties, Mater. Sci. Eng. B Solid-State Mater. Adv. Technol. 231 (2018)

57–65. https://doi.org/10.1016/j.mseb.2018.09.002.

[27] X. Ma, Y.F. Zhao, W.J. Tian, Z. Qian, H.W. Chen, Y.Y. Wu, X.F. Liu, A novel Al matrix composite reinforced by nano-AlN p network, Sci. Rep. 6 (2016) 1–8. https://doi.org/10.1038/srep34919.

[28] M.P. Reddy, F. Ubaid, R.A. Shakoor, A.M.A. Mohamed, Microstructure and Mechanical Behavior of Microwave Sintered Cu50Ti50 Amorphous Alloy Reinforced Al Metal Matrix Composites, JOM. 70 (2018) 817–822. https://doi.org/10.1007/s11837-018-2831-2.

[29] R.K. Sabat, A. Almajid, M. Gupta, S. Suwas, S. Sankaranarayanan, U. Pranav Nayak, Nano-ZnO particle addition to monolithic magnesium for enhanced tensile and compressive response, J. Alloys Compd. 615 (2014) 211–219. https://doi.org/10.1016/j.jallcom.2014.06.163.

[30] M. Bastwros, C. Zhu, G.-Y. Kim, X. Wang, X. Tang, S. Wang, K. Zhang, Effect of ball milling on graphene reinforced Al6061 composite fabricated by semi-solid sintering, Compos. Part B Eng. 60 (2014) 111–118. https://doi.org/10.1016/j.compositesb.2013.12.043.

[31] A. Azarniya, A. Azarniya, A. Abdollah-zadeh, H.R. Madaah Hosseini, S. Ramakrishna, In Situ Hybrid Aluminum Matrix Composites: A Review of Phase Transformations and Mechanical Aspects, Adv. Eng. Mater. 1801269 (2019) adem.201801269. https://doi.org/10.1002/adem.201801269.

[32] B. Kaveendran, G.S. Wang, L.J. Huang, L. Geng, H.X. Peng, In situ (Al3Zr + Al2O3np)/2024Al metal matrix composite with novel reinforcement distributions fabricated by reaction hot pressing, J. Alloys Compd. 581 (2013) 16–22. https://doi.org/10.1016/j.jallcom.2013.06.143.

[33] M. Ao, H. Liu, C. Dong, The effect of La2O3 addition on intermetallic-free aluminium

matrix composites reinforced with TiC and Al2O3 ceramic particles, Ceram. Int. 45 (2019) 12001–12009. https://doi.org/10.1016/j.ceramint.2019.03.093.

[34] G.M. Reddy, M Penchal, Manakari Vyasaraj, Parande Gururaj, Shakoor R.A., Mohamed A.M.A., Structural, mechanical and thermal characteristics of Al-Cu-Li particle reinforced Al-matrix composites synthesized by microwave sintering and hot extrusion, Compos. Part B. 164 (2019) 485–492. https://doi.org/10.1016/j.compositesb.2019.01.063.

[35] M. Rashad, F.S. Pan, A.T. Tang, M. Asif, Effect of Graphene Nanoplatelets addition on mechanical properties of pure aluminum using a semi-powder method, Prog. Nat. Sci. Int. 24 (2014) 101–108. https://doi.org/DOI 10.1016/j.pnsc.2014.03.012.

[36] R. Sankar ganesh, M. Navaneethan, G.K. Mani, S. Ponnusamy, K. Tsuchiya, C. Muthamizhchelvan, S. Kawasaki, Y. Hayakawa, Influence of Al doping on the structural, morphological, optical, and gas sensing properties of ZnO nanorods, J. Alloys Compd. 698 (2017) 555–564. https://doi.org/10.1016/j.jallcom.2016.12.187.

[37] S. Yun, J. Lee, J. Yang, S. Lim, Hydrothermal synthesis of Al-doped ZnO nanorod arrays on Si substrate, Phys. B Condens. Matter. 405 (2010) 413–419. https://doi.org/10.1016/j.physb.2009.08.297.

[38] M. Gupta, W.L.E. Wong, Enhancing overall mechanical performance of metallic materials using two-directional microwave assisted rapid sintering, Scr. Mater. 52 (2005) 479–483. https://doi.org/10.1016/j.scriptamat.2004.11.006.

[39] H. Ahamed, V. Senthilkumar, Consolidation behavior of mechanically alloyed aluminum based nanocomposites reinforced with nanoscale Y2O3/Al 2O3 particles, Mater. Charact. 62 (2011) 1235–1249. https://doi.org/10.1016/j.matchar.2011.10.011.

[40] M.P. Reddy, F. Ubaid, R.A. Shakoor, G. Parande, V. Manakari, A.M.A. Mohamed, M. Gupta, Effect of reinforcement concentration on the properties of hot extruded Al-

Al2O3 composites synthesized through microwave sintering process, Mater. Sci. Eng. A. 696 (2017) 60–69. https://doi.org/1098765432.

[41] V.B. Niste, M. Ratoi, H. Tanaka, F. Xu, Y. Zhu, J. Sugimura, Self-lubricating Al-WS2composites for efficient and greener tribological parts, Sci. Rep. 7 (2017) 1–14. https://doi.org/10.1038/s41598-017-15297-6.

[42] M.P. Reddy, V. Manakari, G. Parande, F. Ubaid, R.A. Shakoor, A.M.A. Mohamed, M. Gupta, Enhancing compressive, tensile, thermal and damping response of pure Al using BN nanoparticles, J. Alloys Compd. 762 (2018) 398–408. https://doi.org/10.1016/j.ympev.2009.07.024.

[43] J. Liu, B. Fernandez, P. Rodriguez, S. Naher, D. Brabazon, Powder processing methodology for production of graphene oxide reinforced aluminium matrix composites, Adv. Mater. Process. Technol. 2 (2016) 437–450. https://doi.org/10.1080/2374068X.2016.1244389.

[44] P.R. Matli, F. Ubaid, R.A. Shakoor, G. Parande, V. Manakari, M. Yusuf, A.M. Amer Mohamed, M. Gupta, Improved properties of Al-Si3N4 nanocomposites fabricated through a microwave sintering and hot extrusion process, RSC Adv. 7 (2017) 34401–34410. https://doi.org/10.1039/c7ra04148a.